

**ELIMINATION OF CONDUCTIVE DIE ATTACH FILM INTERFACIAL DELAMINATION DUE TO INTRINSIC HIGH ASPECT RATIO ULTRATHIN HIGH DIE BOW LEVEL**

**Marty Lorgino D. Pulutan  
Olga S. Rivera**

Backend Technologies  
Ampleon Phils. Inc., Light Industry & Science Park I, Brgy, Diezmo, Cabuyao City, Laguna, 4025  
marty.lorgino.pulutan@ampleon.com, olga.rivera@ampleon.com

**ABSTRACT**

The 0-hour and post reliability interfacial delamination between CDAF and Ag-plated pad was eliminated by surface characterization and diebond process optimization through Six Sigma DMAIC approach. The high intrinsic die bow level of high aspect ratio dies is the main identified factor contributing to the phenomenon inducing peel and other residual stress on the interface. Removal of anti-tarnish content on leadframes, cure profile and bond parameters optimization and rubber tip redesign were the identified solutions to offset the bow level. The anti-tarnish content between the old and new supplied leadframes were determined through Scanning Electron Microscopy (SEM), Elemental Dispersive X-ray (EDX) and Optical Profiling to assess the impact on surface morphology, roughness and compatibility with CDAF material. Simultaneous Thermal Analysis (STA) was done to determine appropriate ramp up rate and soak curing temperature to optimize the curing profile for CDAF and die shear test was performed to assess its effect on adhesion strength improvement. Full factorial Design of Experiment was done to optimize the bond force and bond time for CDAF attach and was correlated with percent delamination taking into account the risk of die crack. Moreover, rubber tip material and design were modified to ensure effective transfer of momentum during diebond which would repress the upward peeling force caused by high bow level. Lastly, all identified solutions were implemented on two consecutive validation builds and the percent delamination both at 0-hour and post reliability readpoints were compared to initial builds using current process settings. The maximum 52% interfacial delamination encountered on initial builds were reduced and completely eliminated to 0% as validated by both post processing image analysis and Scanning Acoustic Microscopy (SAM) percent delamination built-in calculation.

**1. 0 INTRODUCTION**

Ultrathin wafers have intrinsic warpage and bow level due to residual stress during wafer fabrication and the acting gravitational force onto the unsupported weight of the wafer

when placed in cassettes. The induced warpage on the parent wafer slice is translated into component dies during wafer sawing where additional stresses are introduced by the centrifugal force of rotating blade. Not only that high warpage and bow level increases the risk of die chipping and other sawing defects but also contribute to the poor adhesion of the die attach material to the adherend surface especially on the middle region where the maximum point of warpage and bowing is typically situated. The insufficient adhesion forms uneven gap on the interface which triggers non-uniform bondline thickness and consequently causes delamination. Reducing the warpage and bow level of the wafer has been the least option as package assembly process and wafer fabrication are two separate process and that limited solutions on wafer process and handling can be done due to thinness of the die. In this paper, the researchers identified solutions on the CDAF-to-Ag-plated surface interfacial delamination through diebond process optimization and surface characterization to arrive with appropriate leadframe material surface composition and optimized diebond process parameters to offset the peeling stress from deflection of convex curvature of high aspect ratio ultrathin capacitor dies.

**2. 0 REVIEW OF RELATED WORK**

With the continuous drive for miniaturization, semiconductor industry slowly leans towards tight designs requiring material integration with dissimilar properties at high risk of package failure when subjected to high power applications. As such that thermal dissipation should be at high efficiency and that geometry of packaging outlines are becoming complex, dimensions of package components have been modified accordingly to meet the product specifications. Ultrathin wafers and die (with thickness <100  $\mu\text{m}$ ) have been widely used for smaller packages for a lower junction-to-case thermal resistance and increased RF efficiency<sup>1</sup> but are extremely susceptible to crack and have significant bow level and warpage affecting the adherence of die attach on the pad surface which induces interfacial delamination.

In a related study conducted by Tay and Zhu, the effect of varying die thickness on mode mixity and strain energy release rate (ERR) were investigated and showed that die thickness less than 805  $\mu\text{m}$  experience less CTE difference and less ERR thus less risk on die attach to pad delamination but are susceptible to die bending<sup>2</sup>. Aside from the in-process induced bending, the die has intrinsic bow level from residual stresses obtained from wafer fabrication processes such as backside metallization providing tensile stress and backgrinding process giving high compressive stress<sup>1,3</sup>. The bow and warpage level are exacerbated when such fabricated wafers are transferred on cassettes and the gravitational force and weight itself of the material cannot be supported by the normal force with net force unevenly distributed since the wafer edges have support from the stacking. Such phenomenon is common for wafers and die classified as ultra-thin due to gravity-induced deflection. The warpage and bow level from the parent wafer slice will be passed on at die level during wafer dicing where additional stresses are induced. The bow and warpage level of the die would affect the diebond process and output through non-uniform bondline thickness of the die attach material initiating voids and subsequent delamination<sup>4,5</sup>. Banda et al also claimed that die curvature and warpage increase with decreasing thickness of Si die based on surface profiles of 50, 75 and 125  $\mu\text{m}$ <sup>6</sup>.

Several process or material-related issues were primarily delved into as potential contributors to the die attach-to-heatsink delamination. Hoon et. al investigated the potential factors of Type II delamination (die attach-to-die paddle) observed after thermal cycling 2000 cycles and conducted process mapping and rootcause analysis. Die stress modelling showed that thinner die experience lower shear stress along the die attach to die paddle and the bondline thickness and cure profile was further optimized to increase the adhesion of the die attach material to the die paddle surface<sup>7</sup>. On the other hand, Tan claimed that a proper combination of epoxy chemistry and leadframe surface treatment could reduce or eliminate the delamination between die attach and die pad surface after precondition<sup>8</sup> while Prack and Fan attributed the delamination to hygrostress caused by moisture uptake diffusing into gas and releasing vapor pressure during high temperature exposure<sup>9</sup>. Diebond process optimization were also carried out on some studies to mitigate delamination between die attach film (CDAF) to die paddle surface through optimization of scrub cycle, amplitude and bond time<sup>10</sup>.

With numerous studies which dealt with resolution of delamination, only few accounts considered and investigated the effect of die bow and warpage level of varying die sizes on occurrence of delamination and the potential solution such as process optimization to compensate the bow level. Previous study of the researcher showed that the principal stress is higher on the middle region of the die<sup>11</sup> but does not describe the peel stress brought by varying die dimensions

and intrinsic bow level. Also, overmolded packages were assumed to be the usual carriers for previous studies and no research yet was published which used air cavity mold type package as vehicle.

The paper will focus on diebond process optimization to mitigate the observed zero hour and post reliability delamination on conductive die attach film (CDAF) to Ag plated surface interface and to compensate the intrinsic capacitor die warpage and bow level.

### 3.0 METHODOLOGY

The problem-solving data-driven technique used in the study is Define-Measure-Analyze-Improve-Control (DMAIC) process to determine the underlying root causes of observed delamination on the Conductive Die Attach Film (CDAF) to Ag-plated surface interface. At the Define Phase, delamination encountered from previous runs were revisited and remeasured using ImageJ software for quantitative percent calculation and definition of primary metric. On the Measure Phase, potential contributors to the delamination from all involved process steps were considered and categorized using Cause and Effect Analysis and the consistency of delamination percent calculation using ImageJ was assessed through Measurement Systems Analysis (MSA). At the Analyze Phase, risk assessment was done to further trim down the potential factors which will proceed for validation. On-off validation on potential factors related to MOSCAP die material and diebond process parameters were conducted to measure the impact to delamination metric. At the Improve Phase, Design of Experiment (DoE) was performed for diebond parameter settings optimization along with optimized rubber tip design and lastly establishing revised and procedures for post-reliability percent delamination measurement and changes in diebond process parameters to ensure no recurrence of delamination on CDAF to Ag-plated surface interface.

### 4.0 RESULTS AND DISCUSSION

#### 4.1 Define: Quantifying Percent Delamination and Verification Through Cross-Section

Delamination on capacitor dies bonded with CDAF were observed on SCAT images and the percent delamination were measured using ImageJ portable image analysis freeware.



Fig 1. (a) SCAT images of capacitor dies, (b) processed SCAT images on ImageJ showing detected delaminated area and (c) calculated percent delaminated area per die.

Capacitor dies showed gross delamination between CDAF and die paddle surface with calculated percent delamination as high as 52% at 0 hour (after CDAF curing). Almost half of the die area has no contact already with the heatsink and is assumed to propagate across exposure to series of heat processes and reliability. Samples were submitted for cross-section to confirm if delamination is indeed between the die attach material and plated surface.

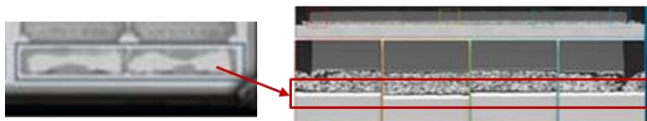


Fig 2. Cross-section of manifested delamination on capacitor die.

Interfacial delamination between the cured CDAF material and Ag-plated surface of the paddle was confirmed on the targeted region where light contrast areas were seen on SCAT image. Such delamination is also observed to increase in size as high as 90% of the die area after precondition and thermal cycling. All sixty units reinspected at SCAT showed presence of delamination on capacitor dies with calculated percentage range between 20 to 55%.

4.2 Measure: Identifying Potential Contributors and Root Cause

From the macro map of the air cavity mold package process flow, the problem solving focused only on the CDAF attach process and the related receivable materials and processes. From the identified involved processes, Cause and Effect Analysis were conducted to determine potential factors classified under Man, Machine, Method, Materials, Measurements and Milieu.

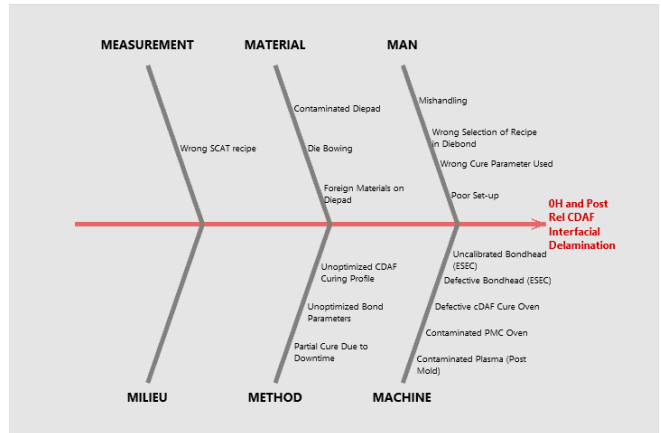


Fig 3. Fishbone diagram of potential factors on the occurrence of CDAF to Ag-plated surface delamination.

The impact of identified 16 factors to the occurrence of delamination were assessed and scored based on relevance to delamination, yield and reliability output. Out of the 16 factors, 7 of which proceeded for risk assessment.

Meanwhile, Measurement Systems Analysis (MSA) was performed to assess the repeatability and reproducibility of the quantification method of delamination through ImageJ using post processed SCAT images. Three operators were instructed to use ImageJ using same set of sampled SCAT images at three trials each.

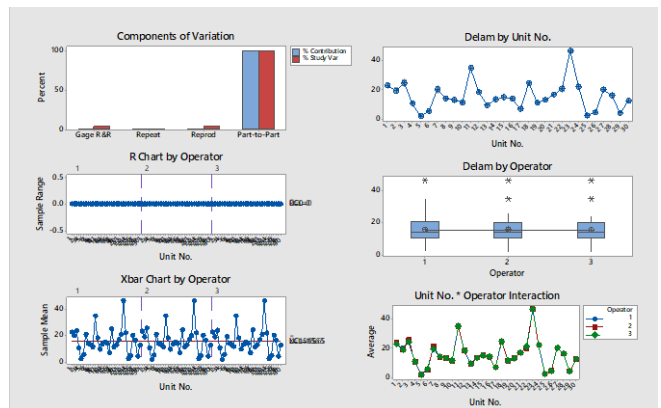


Fig 4. Crossed gage R&R study of percent delamination measurement through ImageJ.

Based on the results, variability associated to repeatability and reproducibility is low and 99.86% of the variation is accounted to part-to-part indicating consistency among repeated trials and different operators using post image processing to quantify percent delamination. R-chart by operator showed points all within control limits which implies that operators measure consistently after repeated trials. The chart also indicates that the procedure established in measuring percent delamination using the freeware would not yield any significant deviation from the true

measurement. Moreover, the delamination by operator chart shows a strong horizontal line across operators indicating that the mean measurements and the distribution of each respective delamination measurements are roughly the same. With the results, the analysis proceeded using the post image processing for quantitative data of total delaminated area per die.

4.3 Analyze: Risk Analysis and Validation of Potential Critical Factors

Failure Modes and Effects Analysis (FMEA) was used to determine the potential critical factors based on the Risk Priority Number (RPN) which is the product of the assessed severity, occurrence and detection per identified failure mode and effect.

Table 1. Identified potential critical factors and respective impact to percent delamination on capacitor die.

No.	Process	Potential Critical Factor	Impact to Metric
1	Material	Presence of anti-tarnish on leadframes	6.67%
2	Material	Intrinsic die bow	(93.33%)
3	Diebond	Unoptimized CDAF curing profile	40%
4	Diebond	Inappropriate rubber tip design	40%
5	Diebond	Unoptimized diebond parameters	13.33%

4.3.1 Critical Factor No. 1: Anti-tarnish Content of Leadframes from Different Suppliers

Using Scanning Electron Microscopy (SEM) in conjunction with Elemental Dispersive X-ray (EDX), the surface morphology and the percent weight of detected Carbon content on the Ag-plated surface were inspected and measured on both old and new leadframe from different suppliers.

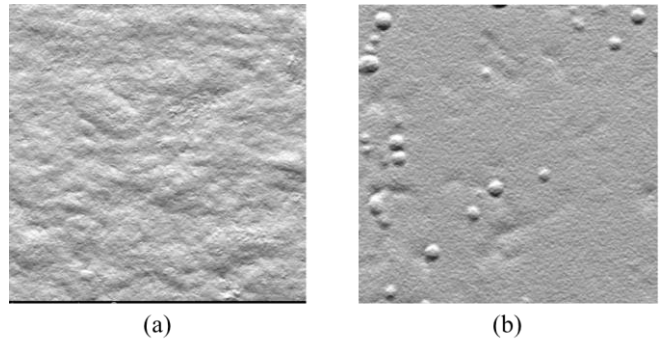


Fig 5. SEM images of (a) old and (b) new leadframe targeted on Ag-plated pad region at 3000x magnification.

The Ag-plated pad on old leadframe appear to have rougher surface than on new leadframe which possess finer surface with fragments of scattered circular bumps. Crevices on the old leadframe are more prominent than on new leadframe which has dominant plateaus with few traces of deeper trenches. Optical profiling was further done to check the difference on the roughness ( $R_a$  and  $R_z$ ) of the two leadframes quantitatively.

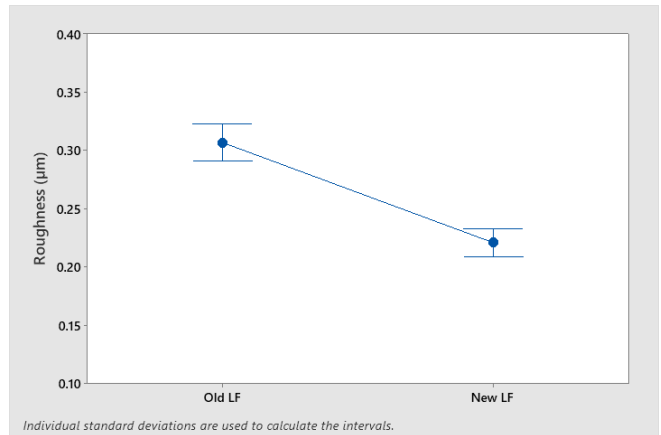


Fig 5.  $R_a$  measured on Ag-plated pad of old and new supplied leadframes.

The two-sample T-test revealed significant difference on both roughness parameter with estimated mean difference of  $0.08577\mu\text{m}$  indicating that the Ag-plated pad on old leadframe is rougher than the new leadframe providing locking mechanism on polymeric matrix of the CDAF material which filled the crevices. However, roughness may not significantly affect the adhesion of CDAF as most epoxy-based materials could provide complete coverage even at micron depth valleys on the surface. The elemental composition on the Ag-plated pad surface was investigated through EDX.

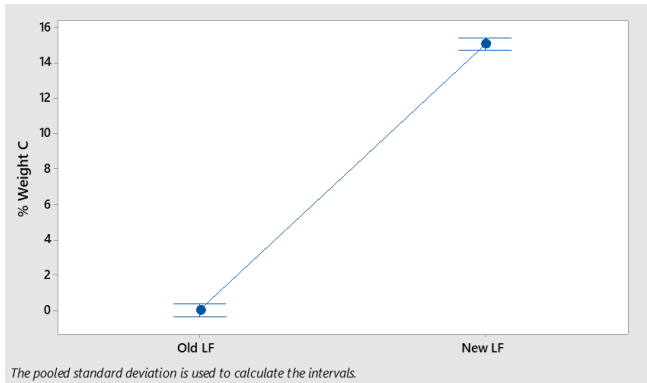


Fig 6. Interval plots of percent weight of detected Carbon content on Ag-plated surface of new and old leadframe.

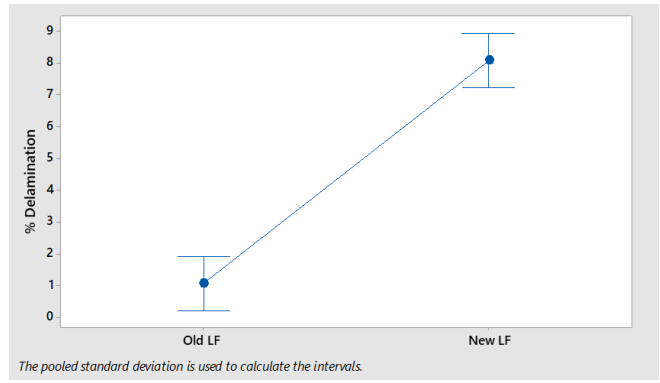


Fig 7. Interval plots of percent delamination on capacitor dies bonded on new and old leadframe.

Using two-sample T-test, the new leadframe from new supplier has a significantly higher Carbon content compared to old samples with 0 to 0.74% Carbon only. The lower roughness on new leadframe may be associated to thicker layer of unremoved anti-tarnish covering the top surface topography structure of the Ag-plated pad. The high Carbon content on the new leadframe is attributed to the anti-tarnish treatment providing 15 to 16% organic components unremoved from as-received samples. The high anti-tarnish might probably not be compatible with the CDAF chemistry compromising the adhesion on the bi-material interface<sup>8</sup>. While the percent delamination measured between the two leadframes are significantly different as shown in Fig. 6, the impact to delamination is only observed on capacitor dies and not on active dies which are relatively larger in dimensions and are also bonded on the same Ag-plated surface. The difference on the response may be attributed on the chemistry of the die attach materials used on the two different types of die – film for passives and Ag sinter epoxy for actives. The higher amount of benzotriazole<sup>10</sup> or derivatives are known to cause paddle delamination and may have different reaction when subjected to heat with conductive die attach film or Ag sinter paste or epoxy. Such correlation is not a scope of the study and the current concentration of benzotriazole detected on new leadframes are assumed to be critical amount to cause poor adhesion of film on Ag-plated pad.

4.3.2 Critical Factor No. 2: Higher Bow Level of High Aspect Ratio Ultrathin Capacitor Dies

As the delamination is only observed on higher aspect ratio capacitor dies, the convex curvature or bow level was measured using Optical 3D Surface Profiler. Bow level is defined as the difference between the minimum and maximum point on the curvature and is expressed as waviness parameter.

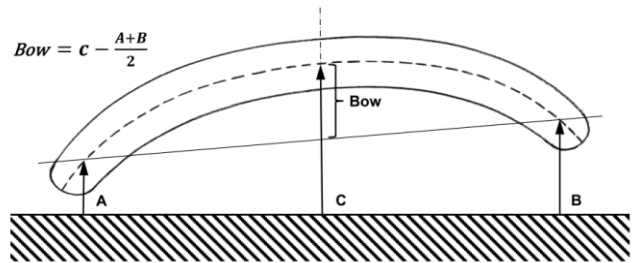


Fig 8. Diagram of bow level measurement<sup>1</sup>.

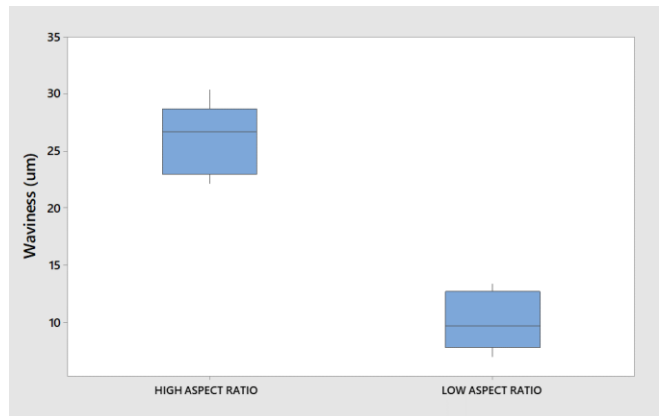


Fig 9. Bow level of high and low aspect ratio capacitor die.

The estimate for difference is 16.23  $\mu\text{m}$  which indicates that the die bow level of high aspect ratio die could be threefold higher than lower aspect ratio. The 3D surface images of the

high aspect ratio dies show high difference between the highest point on the curvature and ends of the die which exhibits the gravity-induced deflection translated from the parent wafer<sup>4,5</sup>. As the dies are received on assembly in wafer form and undergo further stresses during lamination, sawing, and transfer, no further improvement on singulated component die level can be done as such materials are already received as input on succeeding processes particularly on diebond. As such, the peel and other residual stress from high bow level from high aspect ratio capacitors will be offset through diebond parameter optimization.

4.3.3 Critical Factor No. 3: Unoptimized Curing Profile for Increased Adhesion

Based on the data obtained from the previous section, the high aspect ratio dies possess higher bow level which induces both compressive and tensile stress and consequently exerts peel force under the maximum bend stress concentrated along the middle region of the die. Maximum adhesion strength can repress the peel force to prevent separation on the CDAF interface and can be obtained through cure profile optimization.

Dynamic Differential Scanning Calorimetry (DSC) with Thermogravimetric Analysis (TGA) scan at varying ramp up rates (1, 3, 5, 10°C/min.) were performed using approximately 10mg of the CDAF material each run. The peak curing temperature, extrapolated onset of weight loss and percent cure were obtained to optimize the curing profile for the die attach material.

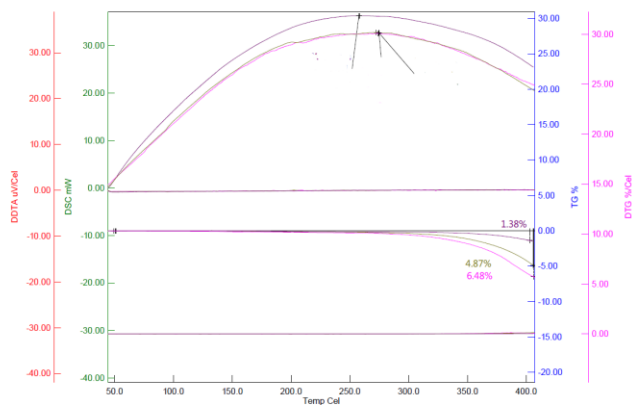


Fig 10. Dynamic heat flow and weight loss curves of CDAF material at 1, 3, 5, 10°C/min.

The peak curing temperature increases with increasing ramp up rate based on the heat flow curves. The peak curing temperature occurs within the range of 190 to 220°C which is higher than the currently released curing profile in the production. The supplier recommendation, however, matches the peak curing temperature and is typically set at the maximum point to allow unreacted species on the B-staged

material to further crosslink. The onset of weight loss however starts near the peak of heat flow curve and is indicative of onset of thermal decomposition, temperature at which should not correspond to the peak curing temperature of the cure profile for the CDAF to prevent material degradation. The peak curing temperature, total percent weight loss and percent cure for the three curing profiles are summarized on Table 2.

Table 2. Comparison of Different Curing Profiles for CDAF.

Cure Profile	Peak Cure Temp. (°C)	Duration (mins.)	% Weight Loss	% Percent Cure
Supplier (TDS)	191 - 200	90 - 100	0.762	99.05
Current	181 - 190	110 - 120	0.688	97.60
Optimized	191 - 200	120 -130	0.801	~100

Optimized curing profile adapted the soak temperature similar to supplier-recommended profile but with longer ramp up and cool down duration to prevent thermomechanical stresses due to difference in Coefficient of Thermal Expansion (CTE). Full crosslinking was attained using optimized curing profile derived from the thermal analysis based on 100% cure degree which triggers maximum adhesion strength. To check the effect of higher cure temperature and longer duration on the adhesion strength of CDAF to Ag-plated pad, die shear test was done using 30 high-aspect ratio passive dies each leg cured at corresponding cure profile based on the table above.

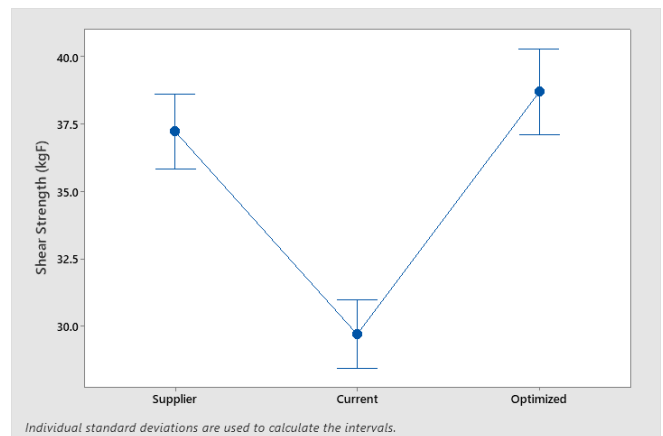


Fig 11. Shear adhesion strength of bonded dies cured using different profiles.

Post hoc test using Tukey Pairwise Comparison was used as a conservative method to determine profiles with significantly different adhesion strength performance than the rest. The current profile yielded significantly lower shear strength than the other two. On the other hand, the supplier-

recommend and optimized curing profile showed no significant difference in adhesion performance indicating that longer ramp up and cool down step does not enhance adhesion of cured CDAF on Ag-plated pad. However, optimized curing profile was still selected to proceed for validation as lower ramp up and cool down rate would minimize the thermomechanical stress in the interface and avoid formation of voids during solvent outgassing<sup>12</sup>.

4.3.4 Critical Factor No. 4: Higher Bond Force and Longer Bond Time

To check the effect of increasing bond time and force on the percent delamination on capacitor dies, 30 units were bonded using high and low bond settings and percent delamination was calculated after curing of CDAF material.

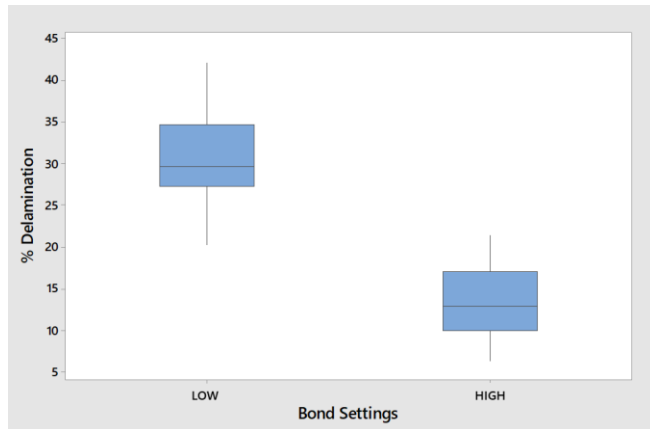


Fig 12. Effect of high and low bond settings on percent delamination on capacitor die.

Using two-sample T-test, there is a significantly different percent delamination between capacitor dies bonded using high and low settings ( $p = 0.000$ ). The estimate for difference is 16.90% which indicates that the high bond settings could significantly improve the delamination on capacitors by approximately 16.90%. However, results also imply that the increased in bond settings alone does not eradicate the delamination completely, which is in disparate with what Capili has reported<sup>10</sup>.

4.3.5 Critical Factor No. 5: Effect of Harder Polyimide Rubber Tip on Percent Delamination

To ensure that transfer of momentum is efficient from tip down to heatsink which would allow CDAF in full contact to Ag-plated surface driven by compressive stress, the effect of harder plastic polyimide rubber tip compared to existing was investigated using low bond settings.

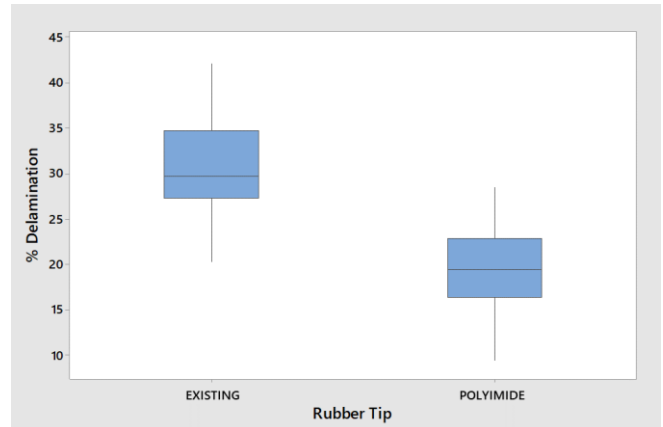


Fig 13. Percent delamination of units bonded using existing and polyimide rubber tip.

Distribution shows that the minimum up to the Q1 of percent delamination bonded using existing rubber tip is approximately the same with Q3 to maximum of measured delamination of units bonded using harder polyimide rubber tip material. The IQR of the new rubber tip however, is significantly lower than on existing rubber tip suggesting that the percent delaminated area on capacitor dies was significantly reduced as backed up by the results of two sample t-test ( $p = 0.000$ ). The estimate for difference is 10.83% indicating that the harder polyimide rubber tip material could significantly reduce the delamination by 10.83%. The results also imply that the use of harder plastic material on rubber tip would efficiently transfer the bond force to the die suppressing the peak point of the curvature allowing full contact of laminated CDAF on the Ag-plated surface. Nevertheless, a considerable amount of percent delamination is still present at 0 hour and further optimization is still needed to completely remove the observed delamination on CDAF-to-Ag-plated surface interface.

4.4 Improve: Bond Parameter and Rubber Tip Design Optimization

As significant amounts of Carbon were detected on the die paddle area, the anti-tarnish process on the supplier was skipped to prevent deposition of organic contaminants unremoved during diebond. Anti-tarnish-free leadframes were used on the succeeding trials to eliminate the contribution of high Carbon content.

Table 3. Design of Experiment Matrix to Determine Optimum Bond Force and Bond Time.

Leg No.	Bond Force (N)	Bond Time (ms)
1	Low	Low
2	Mid	Low
3	High	Low
4	Low	Mid
5	Mid	Mid
6	High	Mid
7	Low	High
8	Mid	High
9	High	High

Based on General Full Factorial DoE, both bond time and bond force influence the measured percent delamination on capacitor die at 0 hour ( $p = 0.000$ ) but the interaction of the two parameters is non-significant. Optimized parameters are high bond force and high bond time which would reduce the percent delamination by approximately to 11% as illustrated on Fig. 11.

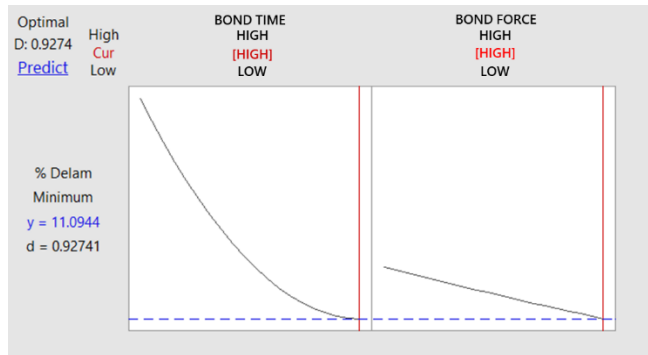


Fig 14. Optimization plot of bond force and time in response of percent delamination.

However, optimum bond force and time are beyond the specifications limit of the current diebond process and hence would have high risk for die crack. Since post hoc tests (both Tukey and Fisher Pairwise Comparison) showed no significant difference between low or mid bond force in combination with high bond time to the optimum parameters. The low bond force at high bond time is the selected set of diebond parameter to minimize delamination at low risk of die crack.

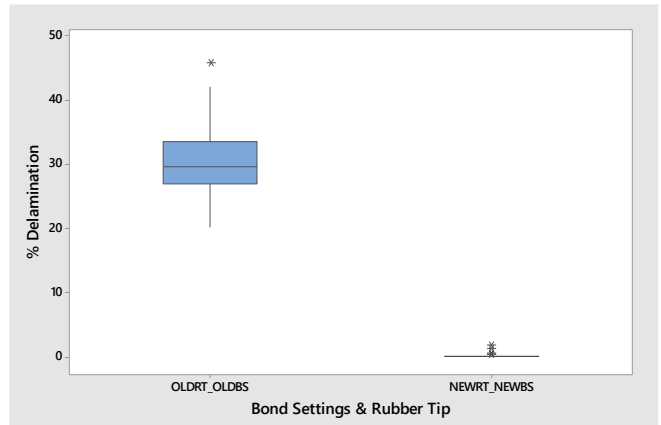


Fig 15. Percent delamination of units bonded using existing rubber tip with old bond settings and reduced size rubber tip with optimum bond settings.

The rubber tip design was further optimized by reducing the die contact coverage from 90-95% to 80% to target and provide more compressive stress on the highest curvature points and lessen the deflection from the die edges. Based on the results, percent delamination on capacitor die at 0 hour was reduced to about 0% when new rubber tip design using harder polyimide material in combination with optimum bond settings and anti-tarnish-free leadframe were implemented.

4.5 Control: Implementation of Process and Material Developments

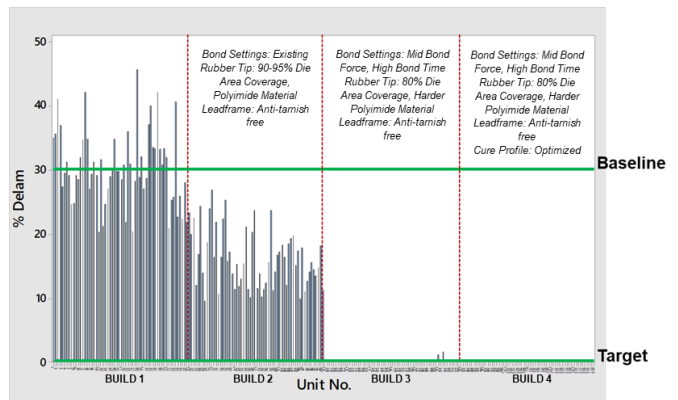


Fig 16. Percent delamination of 30 sampled units per build and implemented process and material developments.

The use of optimum bond parameters, reduced die area coverage and rubber tip material, anti-tarnish-free leadframes and optimized cure profile were implemented on succeeding builds and 60 units were sampled for SCAT imaging to measure the percent delamination on the high aspect ratio capacitor die component.

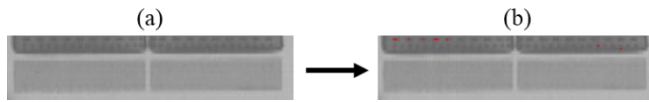


Fig 17. Post processing of SCAT image using ImageJ to measure the percent delamination.

No delamination was detected along the CDAF-to-Ag-plated interface on capacitor dies after implementation of process and material improvements. The percent delamination was reduced from around 50% to 0% even after exposure to 1000 cycles of thermal cycling.

### 5.0 CONCLUSION

In summary, two main factors were demonstrated to contribute on the occurrence of CDAF-to-Ag-plated surface delamination – high anti-tarnish content of the leadframe and the intrinsic bow level of thin capacitor dies. The high aspect ratio thin capacitor dies showed intrinsic bow level as high as 30  $\mu\text{m}$  and were offset through cure profile, bond parameter and rubber tip design optimization. Optimized curing profile with higher soak temperature and lower ramp up and cool down rates have shown to increase adhesion strength of CDAF to Ag-plated pad while minimizing thermomechanical stress induced by rapid ramp up rate. High bond force and long bond time had the highest reduction in percent delamination but are deemed to be at high risk for die crack since such values are beyond the established specifications limit. Since the difference in percent delamination reduction between high and low bond force with high bond time is insignificant, the low bond force was selected for CDAF diebond process. The polyimide material and reduced die area coverage for rubber tip were also found to decrease the percent delamination. Implementing the process and material improvements – anti-tarnish free leadframes, optimized cure profile, optimum bond settings and redesigned rubber tip eliminated the delamination at 0 hour and until 1000 cycles of thermal cycling. The results imply that the delamination brought by intrinsic bow level of high aspect ratio die can be countervailed through process optimization while considering other potential factors such as material variation at least possible.

### 6.0 RECOMMENDATIONS

To assess the effect of material variation on the occurrence of delamination associated to high bow level of thin dies, the researchers suggest to check different CDAF material with different material property such as adhesion strength, CTE and modulus. The effect of different plating surface and treatment on the percent delamination is also recommended to determine the appropriate plating chemistry on the adhesion of CDAF which would also quell the peeling effect of intrinsic bow level of the die. Lastly, different die sizes

should also be explored to correlate and establish a mathematical model which would describe and predict the warpage and bow level in relation to die dimension and aspect ratio.

### 7.0 ACKNOWLEDGMENT

The authors would like to express their sincerest gratitude to Backend Technologies Competence Center engineers and technicians who help execute the experiments and to Ampleon Phils. Inc. management team for the support which made the study possible.

### 8.0 REFERENCES

1. M. R. Marks, et.al., *IEEE Transactions on Components, Packaging and Manufacturing Technology*, 4, 12, 2014, 2042-2057.
2. H. Zhu, *52nd Electronic Components and Technology Conference 2002 (Cat. No.02CH37345)*, 2002, 199-204.
3. A. S. Francomacaro, et. al., *2009 59th Electronic Components and Technology Conference*, 2009, 574-584.
4. V. Wen Sheng, et. al., *2006 8th Electronics Packaging Technology Conference*, 2006, 837-842.
5. M. K. Grief and J. A. Steele, *Nineteenth IEEE/CPMT International Electronics Manufacturing Technology Symposium*, 1996, 190-194.
6. C. Banda, et. al., *IEEE Transactions on Electronics Packaging Manufacturing*, 31, 1, 2008, 1-8.
7. K. L. Hoon, et.al., *2013 IEEE 15th Electronics Packaging Technology Conference (EPTC 2013)*, 2013, 549-554.
8. T. C. King, *2006 Thirty-First IEEE/CPMT International Electronics Manufacturing Technology Symposium*, 2006, 370-375.
9. E. R. Prack and X. Fan, *2006 IEEE International Symposium on Semiconductor Manufacturing*, 2006, 219-222.
10. M. D. Capili, *International Research Journal of Advanced Engineering and Science*, 4, 4, 2019, 319-322.
11. B. J. Villacarlos and M. L. D. Pulutan, *2020 IEEE 22nd Electronics Packaging Technology Conference (EPTC)*, 2020, 307-311.
12. C. Weber, et. al., *2015 IEEE 65th Electronic Components and Technology Conference (ECTC)*, 2015, 1866-1873.